

Viscous Transonic Decretion in Disks of Be Stars

Atsuo T. OKAZAKI

*Faculty of Engineering, Hokkai-Gakuen University, Toyohira-ku, Sapporo 062-8605**E-mail: okazaki@elsa.hokkai-s-u.ac.jp*

(Received ; accepted)

Abstract

We study the characteristics of the outflow in disks of Be stars, based on the viscous decretion disk scenario. In this scenario, the matter ejected from the equatorial surface of the star drifts outward because of the effect of viscosity, and forms the disk. For simplicity, we adopt the α -prescription for the viscous stress, and assume the disk to be isothermal. Solving the resulting wind equations, we find that a transonic solution exists for any value of α . The sonic point is located at $r > 100R$ for plausible values of parameters, where R is the stellar radius. The sonic radius is smaller for higher temperature and/or larger radiative force. We also find that the topology of the sonic point is nodal for $\alpha \gtrsim 0.95$, while it is of saddle type for $\alpha \lesssim 0.9$. We expect that the sonic point in the former case is unstable, whereas that in the latter case is stable. The outflow is highly subsonic in the inner part of the disk. Roughly, the outflow velocity increases linearly with r and the surface density decreases as r^{-2} . Interestingly, the disk is near Keplerian in the inner subsonic region, while it is angular momentum conserving in the outer subsonic region and in the supersonic region. Our results, together with the observed range of the base density for Be star disks, suggest that the mass loss rate in the equatorial region is at most comparable with that in the polar region.

Key words: hydrodynamics — radial velocity — stars: Be — stars: mass loss — stars: winds

1. Introduction

Be stars are non-supergiant early-type stars with Balmer emission lines, whose spectral types range from late O- to early A-type. Extensive studies have revealed that a Be star has a two-component extended atmosphere, a polar region and a cool ($\sim 10^4$ K) equatorial disk. The polar region consists of a low-density, fast outflow emitting UV radiation. The terminal velocity of the polar wind is of the order of 10^3 km s $^{-1}$. The wind structure is well explained by so-called line-driven wind model, in which the radiative acceleration results from the scattering of the stellar radiation in an ensemble of spectral lines (Castor et al. 1975; Abbott 1982). The mass loss rate of this region inferred from the UV lines is about $10^{-11} - 10^{-9} M_{\odot} \text{ yr}^{-1}$ (Snow 1981).

On the other hand, the equatorial disk consists of a high-density plasma from which the optical emission lines and the IR excess arise. The radial velocity of the disk is smaller than a few km s $^{-1}$, at least within ~ 10 stellar radii (Hanuschik 1994, 2000; Waters, Marlborough 1994). The small radial velocity and the small pressure gradient force, as in viscous accretion disks, suggest that the equatorial disk is pressure-supported and geometrically thin in the vertical direction and is rotationally-supported in the radial direction. In fact, the presence of near Keplerian disks around Be stars is supported observationally as well as theoretically. For example, the relation between

the size of the H α -emitting region of Be disks resolved with the optical interferometer (Quirrenbach et al. 1997) and the separation of the double peaks of the H α line is in agreement with that expected for near Keplerian disks. In addition, the long-term line-profile variations are well explained by global disk oscillations with a one-armed density perturbation pattern, which can be present only in near Keplerian disks (Okazaki 1991; Papaloizou et al. 1992; Hanuschik et al. 1995). The mass loss rate through the disk is not known. The density in the disk derived from the IR excess and the observed upper limit of the radial velocity impose the upper limit of the mass loss rate of several $\times 10^{-9} M_{\odot} \text{ yr}^{-1}$ (Waters, Marlborough 1994).

At present, the viscous decretion disk model proposed by Lee et al. (1991) is the only model that naturally yields near Keplerian disks around Be stars. In this model, matter supplied from the equatorial surface of the star gradually drifts outward by the viscous torque and forms the disk. Assuming Keplerian rotation and neglecting the advective term in the equation of motion, Lee et al. (1991) obtained steady and thermally-stable structure of viscous decretion disks around Be stars.

Later, using a 3D Smoothed Particle Hydrodynamics code, Kroll and Hanuschik (1997) studied the evolution of the gas ejected temporarily from a Be star to model the transient disk formation/decay process around μ Cen. They found that the gaseous particles gradually expand

and form a near Keplerian disk in the viscous timescale.

These works show that the viscous torque is likely the agent that makes a disk near Keplerian. However, since the specific angular momentum in the near Keplerian disk increases with radius, Be disks are unlikely near Keplerian far from the star. A general belief is that the disk which is Keplerian near the star becomes angular momentum conserving far from the star, although no theoretical or observational study has confirmed this transitional feature of Be disks.

The purpose of the present paper is to investigate whether Be disks have this transitional feature, based on the viscous decretion disk scenario. In section 2, we describe the disk model and formulate the eigenvalue problem for obtaining the radial structure of viscous decretion disks. We present the transonic solutions and discuss the topology of the sonic points in section 3. In section 4, we draw our conclusions and discuss several issues which remain unsolved.

2. Basic Equations for Viscous Decretion Disks

We assume that the circumstellar disk of a Be star is steady, geometrically thin, and symmetric about the rotational axis and the equatorial plane. For simplicity, we adopt the Shakura-Sunyaev's prescription for the viscous stress. Since the deviation from a point mass potential due to the rotational distortion of the star is small in general, we neglect the quadrupole contribution to the gravitational potential. We use a cylindrical coordinate system (r, ϕ, z) to describe the disk.

Millar and Marlborough (1998, 1999) computed the temperature distribution within $100R$ around the B0 star γ Cas and the B8-9 star 1 Del by balancing at each position the rates of energy gain and energy loss, where R is the stellar radius. They found that the disk temperature is roughly constant in the radial direction within $100R$. Since solving the hydrodynamical equations together with the energy equation is a formidable task, we assume for simplicity that the disk is isothermal. We believe that this assumption is a reasonable one as a first step to model the disk.

Under these assumptions, the vertically-integrated equations describing the mass, momentum, and angular momentum conservation in the disk around the star of mass M , together with the equation of state and the Shakura-Sunyaev viscosity prescription, are

$$\dot{M} + 2\pi r V_r \Sigma = 0, \quad (1)$$

$$-V_r \frac{dV_r}{dr} + \frac{V_\phi^2}{r} - \frac{GM}{r^2} - \frac{1}{\Sigma} \frac{dW}{dr} + F_{\text{rad}} + \frac{3W}{2r\Sigma} = 0, \quad (2)$$

$$V_r \frac{dV_\phi}{dr} + \frac{V_r V_\phi}{r} - \frac{1}{r^2 \Sigma} \frac{d}{dr} (r^2 t_{r\phi}) = 0, \quad (3)$$

$$W = c_s^2 \Sigma, \quad (4)$$

$$t_{r\phi} = -\alpha W, \quad (5)$$

where \dot{M} is the decretion rate, Σ , W , and $t_{r\phi}$ are the vertically-integrated density, pressure, and r - ϕ component of the viscous stress, respectively, V_r and V_ϕ are the radial and azimuthal components of the vertically-averaged velocity, respectively, F_{rad} is the vertically-averaged radiative force per unit mass, c_s is the isothermal sound speed, and α is the viscosity parameter. The last term of the left-hand-side of equation (2) is the correction for the decrease of radial component of the effective gravity away from the equator (e.g., Matsumoto et al. 1984).

Since the radial flow in the inner part of viscous decretion disks is considered to be highly subsonic (Lee et al. 1991), the radiative acceleration would arise not from the optically-thick strong lines but from optically-thin weak lines (and from the optically-thin continuum). Since almost nothing is known about the form of the radiative force due to an ensemble of optically-thin lines, we adopt in this paper the parametric form used by Chen and Marlborough (1994):

$$F_{\text{rad}} = \frac{GM\Gamma}{r^2} + \frac{GM(1-\Gamma)}{r^2} \eta \left(\frac{r}{R}\right)^\epsilon, \quad (6)$$

where η and ϵ are parameters which characterize the force due to the ensemble of optically-thin lines. In the above expression, Γ is the Eddington factor that accounts for the reduction in the effective gravity due to electron scattering. In the rest of this paper, we neglect the Eddington factor Γ , because for typical values for Be stars, Γ is as small as ~ 0.03 for a B0V star and ~ 0.003 for a B5V star. The radiative force is then written as

$$F_{\text{rad}} \simeq \frac{GM}{r^2} \eta \left(\frac{r}{R}\right)^\epsilon. \quad (7)$$

Eliminating W , Σ , and $t_{r\phi}$ from equations (1)–(3), we obtain the following equations which describe the steady viscous flow:

$$\left(V_r - \frac{c_s^2}{V_r}\right) \frac{dV_r}{dr} = g_{\text{eff}} + \frac{\ell^2}{r^3} + \frac{5}{2} \frac{c_s^2}{r}, \quad (8)$$

$$\ell = \ell_s + \alpha c_s^2 \left(\frac{r_s}{c_s} - \frac{r}{V_r}\right), \quad (9)$$

where g_{eff} is the effective gravity defined by

$$g_{\text{eff}} = -\frac{GM}{r^2} + F_{\text{rad}} \simeq -\frac{GM}{r^2} \left[1 - \eta \left(\frac{r}{R}\right)^\epsilon\right], \quad (10)$$

$\ell = rV_\phi$ is the specific angular momentum, and r_s and ℓ_s are the radius of the sonic point and the specific angular momentum at the sonic point, respectively. It is important to note that the angular momentum distribution of

the flow is not given a priori but obtained, with the radial velocity distribution, as the solution of equations (8) and (9). In these equations, r_s and ℓ_s are the eigenvalues. Note also that, from equation (9), which indicates $\ell + \alpha c_s^2 r / V_r$ is constant, V_r has to approximately linearly increase with r in order for the disk to be near Keplerian.

We solve equations (8) and (9) by the shooting method with the starting point at $r = R$. Each trial integration needs two starting values, one of which is freely specifiable. We specify V_r as a freely specifiable starting value and choose ℓ so as to be consistent with these equations in the very vicinity of $r = R$.

3. Viscous Transonic Solutions

Wind equations (8) and (9) include five independent parameters which characterize the solution. They are the viscosity parameter α , the isothermal sound speed c_s , the star's break-up velocity $(GM/R)^{1/2}$, and the radiative parameters η and ϵ . Since, in our model, the disk is assumed to be isothermal, the structure of the viscous transonic outflow is independent of the mass accretion rate \dot{M} [see section 3 of Abramowicz and Kato (1989)]. Solving equations (8) and (9) for a wide range of these parameters, we found that a transonic solution exists for any combination of parameter values.

In the first part of this section, we discuss the structure of viscous transonic accretion disks. In the second part, we discuss the topology of the sonic point. Since we found that the accretion disk structure is not sensitive to the spectral type of the central star, we will present only examples in which the central star is a B0 main-sequence star with $M = 17.8 M_\odot$, $R = 7.41 R_\odot$, and $T_{\text{eff}} = 2.80 \cdot 10^4 \text{ K}$ (Allen 1973), where T_{eff} is the effective temperature.

3.1. Structure of the Viscous Transonic Outflow

Figure 1 shows the structure of the viscous transonic accretion disk for $T_d = \frac{1}{2} T_{\text{eff}}$ and $(\eta, \epsilon) = (0, 0)$, where T_d is the disk temperature. In figure 1, solid, dashed, and dash-dotted lines denote V_r/c_s , $V_\phi/(GM/R)^{1/2}$, and $\Sigma/\Sigma(R)$, respectively. For comparison purpose, transonic solutions for $\alpha = 1$ (thick lines), $\alpha = 0.1$ (lines with intermediate thickness), and $\alpha = 0.01$ (thin lines) are shown.

From figure 1, we find that the sonic point is located far from the star and the outflow is highly subsonic for $r \ll 10^2 R$. We also find that physical quantities vary approximately as $V_r \propto r$, $\Sigma \propto r^{-2}$ (i.e., the local density $\propto r^{-7/2}$ in the isothermal disk), and $V_\phi \propto r^{-1/2}$ in the inner subsonic part. For smaller α , the slopes of V_r and Σ become steeper in the outer subsonic part. In the outer subsonic part and in the supersonic part, V_ϕ approximately decreases as r^{-1} . It is important to note

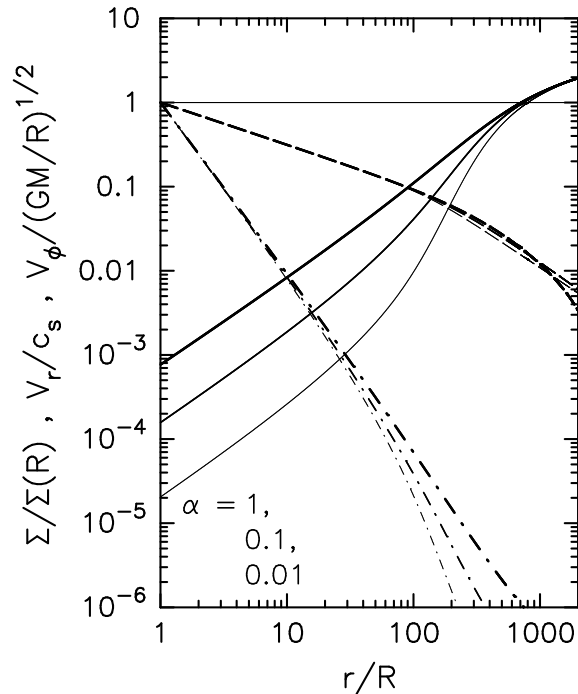


Fig. 1.. Structure of the viscous transonic accretion disk for $T_d = \frac{1}{2} T_{\text{eff}}$ and $(\eta, \epsilon) = (0, 0)$. The central star is a B0 main-sequence star. Solid, dashed, and dash-dotted lines denote V_r/c_s , $V_\phi/(GM/R)^{1/2}$, and $\Sigma/\Sigma(R)$, respectively. Thick lines, lines with intermediate thickness, and thin lines are for $\alpha = 1, 0.1,$ and 0.01 , respectively.

that the transonic accretion disk has the transitional feature mentioned in section 1: It is near Keplerian in the inner part, while it is angular momentum conserving in the outer part. As shown below, these features of viscous transonic accretion disks hold irrespective of parameter values.

As mentioned above, there are five parameters that characterize the current problem. In figure 1 we have studied how the viscosity parameter affects the transonic solution with the other four parameters being fixed. In figure 2, we show how transonic solutions depend on (a) the disk temperature T_d/T_{eff} and (b) the radiative parameters η and ϵ . From figure 2, we note that the characteristics of the transonic solutions are always the same as those shown in figure 1. We also note that the sonic radius is smaller for higher disk temperature and/or larger radiative force.

It is important to note that it is basically the pressure force that accelerates the flow up to a supersonic speed. The acceleration by the pressure force does not work effectively in the region where it is much weaker than the effective gravity. This is why the sonic point is

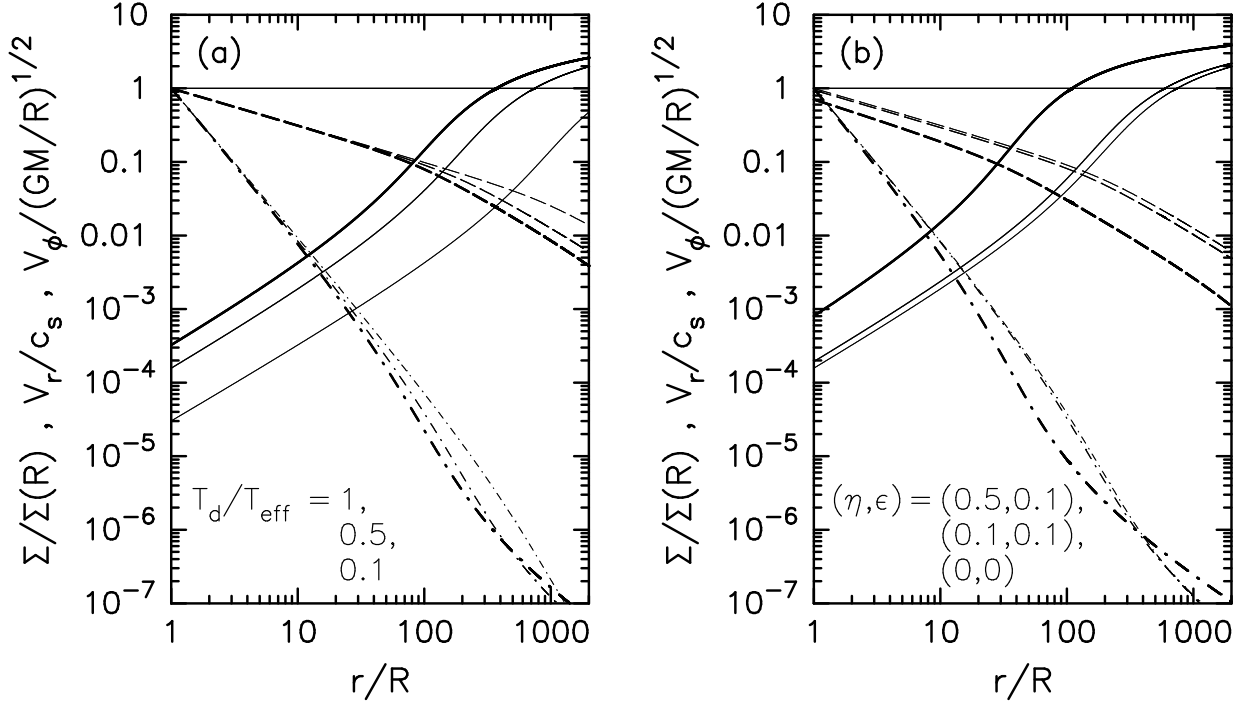


Fig. 2.. Parameter dependence of the viscous transonic solutions. The value of α is fixed to be 0.1. The central star is a B0 main-sequence star. (a) The temperature dependence: Thick lines, lines with intermediate thickness, and thin lines are for $T_d/T_{\text{eff}} = 1, 1/2,$ and $1/10,$ respectively. No radiative force is included. (b) The dependence on the radiative parameters: Thick lines and lines with intermediate thickness are for $(\eta, \epsilon) = (0.5, 0.1)$ and $(\eta, \epsilon) = (0.1, 0.1),$ respectively. Thin lines are for no radiative force. The disk temperature is fixed to be $T_d/T_{\text{eff}} = 1/2.$ Other format of the figure is the same as that of figure 1.

located far from the star. From equation (8), the sonic radius r_s is roughly given by $r_s \sim \frac{2}{5}GM/c_s^2$ when the radiative force is much weaker than gravity. That the pressure force plays an important role for the acceleration suggests that the flow structure can be sensitive to the radial distribution of the disk temperature. We have assumed, for simplicity, the disk to be isothermal, but the disk temperature should be originally determined by solving the energy equation. If the disk is not isothermal, it will affect the flow structure, in particular in the region of $r > 100R,$ where the sonic point in the isothermal disk lies.

We would like to make a brief comment here on the radial velocity of viscous decretion disks. One may estimate from equation (3) that the radial velocity V_r is of the order of $\alpha(H/r)^2V_\phi,$ which is reduced to $0.6\alpha(T_d/T_{\text{eff}})(r/R)^{1/2} \text{ km s}^{-1}$ for an isothermal, near Keplerian disk around a B0-type main-sequence star. As shown in figures 1 and 2, however, this estimate is wrong in both absolute magnitude and radial dependence. Equation (9) indicates that V_r roughly linearly increase with $r,$ as discussed at the end of section 2, and has to be much smaller than $\alpha(H/r)^2V_\phi$ near the star.

3.2. Topology of the Sonic Point

It is well known that the stability of the transonic accretion with Shakura-Sunyaev viscosity prescriptions is related to the topology of the sonic point (e.g., Abramowicz, Kato 1989, and references therein). For α smaller than a critical value, the sonic point is of saddle type and the transonic accretion is stable. On the other hand, for α greater than the critical value, the sonic point is nodal and the transonic accretion becomes unstable. The instability arises as a result of work done by viscous force [see Kato et al. (1988) for detailed analysis].

In the current model, both left-hand and right-hand sides of equation (8) must vanish at the sonic point, i.e.,

$$V_r(r_s) = c_s, \quad (11)$$

$$\ell_s^2 = GMr_s \left[1 - \eta \left(\frac{r_s}{R} \right)^\epsilon \right] - \frac{5}{2}c_s^2r_s^2. \quad (12)$$

To examine the topology of the sonic point, we evaluate the derivative dV_r/dr at $r = r_s.$ After some manipula-

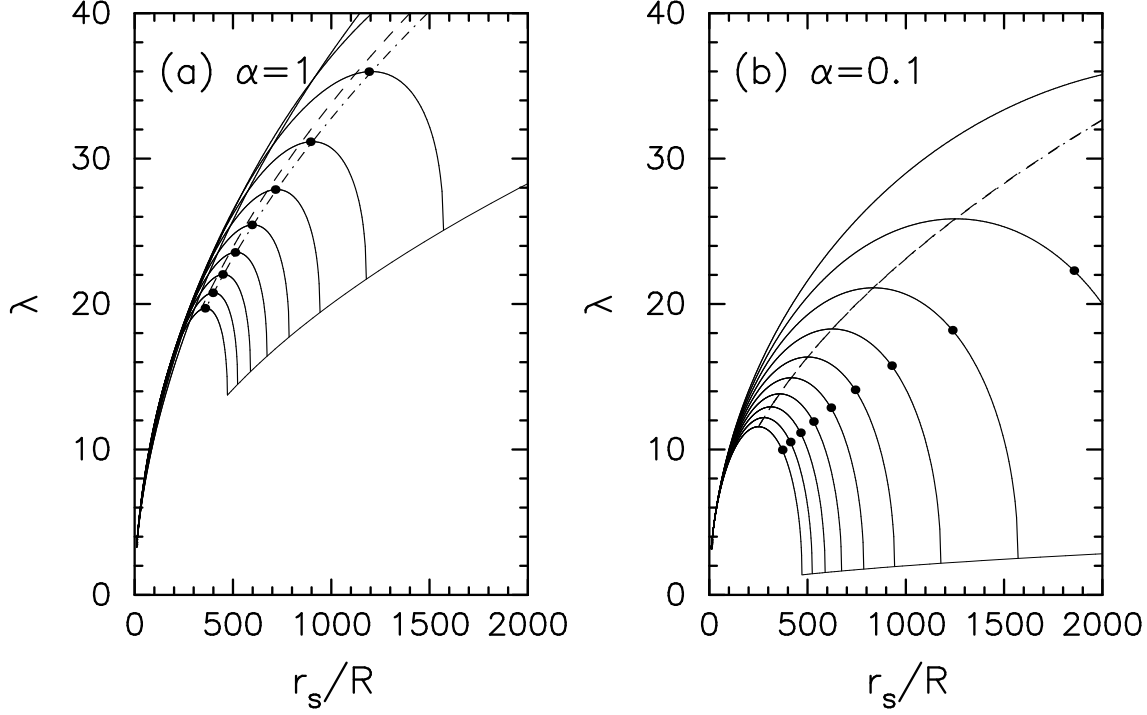


Fig. 3.. Diagram showing the location of the sonic points in the (r_s, λ_s) -plane for (a) $\alpha = 1$ and (b) $\alpha = 0.1$. No radiative force is included and $\lambda_s = \ell_s + \alpha c_s r_s$ is normalized by $(GMR)^{1/2}$. The central star is a B0-type main-sequence star. Each contour denotes the relation between r_s and λ_s for a constant sound speed. From the bottommost curve upwards, $T_d/T_{\text{eff}} = 1, 0.9, 0.8, \dots, 0.3, 0.2$, and 0.1 . The filled circle on each contour indicates the position of the sonic point. In each panel, the dashed line separates the spiral-type sonic point region (upper side of the line) from the nodal-type sonic point region (lower side of the line), and the dash-dotted line separates the nodal-type region (upper side) from the saddle-type region (lower side). In figure 3b the nodal-type region is so narrow that it is indistinguishable on the figure. The thin solid line in each panel indicates a boundary in the (r_s, λ_s) -plane, below which the circular orbit at the sonic radius is unstable.

tions, we have

$$\left. \frac{dV_r}{dr} \right|_{r_s} = \frac{\alpha \ell_s}{2r_s^2} \pm \left(\frac{\alpha^2 \ell_s^2}{4r_s^4} - X \right)^{1/2}, \quad (13)$$

where

$$X = -\frac{2GM}{r_s^3} \left[1 - \eta(2 - \epsilon) \left(\frac{r_s}{R} \right)^\epsilon \right] + \frac{3}{2} \frac{\ell_s^2}{r_s^4} + \frac{\alpha c_s \ell_s}{r_s^3} + \frac{5}{4} \frac{c_s^2}{r_s^2}. \quad (14)$$

Note that equations (13) and (14) are quite similar to equations (2.15) and (2.16) of Abramowicz and Kato (1989) for the transonic accretion. According to the standard classification of critical points (e.g., Ferrari et al. 1985), the sonic point is of saddle type if $X < 0$, nodal if $0 < X < \alpha^2 \ell_s^2 / 4r_s^4$, and spiral if $X > \alpha^2 \ell_s^2 / 4r_s^4$.

In figure 3, as typical examples, we present the location of the sonic points for (a) $\alpha = 1$ and (b) $\alpha = 0.1$. In the figure, $\lambda_s \equiv \ell_s + \alpha c_s r_s$ is normalized by $(GMR)^{1/2}$. Solid contours denote the relation between r_s and λ_s , given by equation (12), for $T_d/T_{\text{eff}} = 1, 0.9, 0.8, \dots, 0.3, 0.2$,

and 0.1 from the bottom to the top. The filled circle on each contour indicates the position of the sonic point. In each panel, the dashed line separates the spiral-type sonic point region (upper side of the line) from the nodal-type sonic point region (lower side of the line), and the dash-dotted line separates the nodal-type region (upper side) from the saddle-type region (lower side). In figure 3b the nodal-type region is so narrow that it is indistinguishable on the figure. The thin solid line in each panel indicates a boundary in the (r_s, λ_s) -plane, below which the circular orbit at the sonic radius is unstable.

Figure 3 shows that the sonic point for $\alpha = 1$ is located in the nodal-type region, whereas that for $\alpha = 0.1$ is in the saddle-type region. Examining the transonic solutions for a wide range of parameters, we found that the topology of the sonic point depends only on α and there is a critical value, α_* , such that the sonic point is nodal for $\alpha > \alpha_*$, while it is of saddle type for $\alpha < \alpha_*$. Note the similarity between the transonic decretion and accretion. In our model, α_* lies between 0.9 and 0.95. This means that the steady transonic decretion in disks of Be

stars exists for $\alpha \lesssim 0.9$, whereas the transonic decretion cannot be steady for $\alpha \gtrsim 0.95$.

4. Summary and Discussion

We have examined the characteristics of the outflow in viscous decretion disks around Be stars. For simplicity, we have assumed the disk to be isothermal and adopted the Shakura-Sunyaev α -prescription for the viscous stress. As the radiative force, we have adopted the parametric form used by Chen and Marlborough (1994).

Solving the resulting wind equations for a wide range of parameter values, we have found that a transonic solution exists for any combination of parameters. When the radiative force is much smaller than the gravity, it is basically the pressure force that accelerates the flow up to a supersonic speed. The sonic radius r_s is, then, roughly given by $r_s \sim \frac{2}{5}GM/c_s^2$. The sonic radius is smaller for higher disk temperature. A larger radiative force also gives a smaller sonic radius. The outflow is highly subsonic in the inner part of the disk. Approximately, the radial velocity increases as r and the surface density decreases as r^{-2} in the inner subsonic part. For smaller α , slopes of these quantities become steeper in the outer subsonic part. Interestingly, the disk is near Keplerian ($V_\phi \sim r^{-1/2}$) in the inner subsonic part, while it is angular momentum conserving ($V_\phi \sim r^{-1}$) in the outer subsonic part and in the supersonic part.

We have also found that the topology of the sonic point is nodal for α greater than a critical value, α_* , whereas it is of saddle type for $\alpha < \alpha_*$. In our model, α_* lies between 0.9 and 0.95 irrespective of values of other parameters. From the similarity between the physics of accretion and decretion and the study of the transonic accretion disks, we expect that the transonic decretion disks with $\alpha < \alpha_*$ are stable, whereas those with $\alpha > \alpha_*$ are unstable.

We have seen that the viscous transonic decretion disks have many characteristics in agreement or consistent with the observed features. Thus, the current model is satisfactory as a first step to obtain a sophisticated model of Be disks. We have to admit, however, that there are several issues which remain unsolved by the current version of the model. They are the observed high mass-loss rate through the disk or short disk-formation timescale, a variety of the observed density distribution, and the mass supply mechanism from the star. We would like to discuss these issues in the rest of this paper.

First, we consider the mass loss rate $|\dot{M}|$ through the disk. In principle, the mass loss rate is determined by how much torque is exerted by the star at the inner disk boundary. Unfortunately, however, we have no satisfactory model for the star-disk interaction or observational estimate of $|\dot{M}|$ in quasi-steady disks ($|\dot{M}|$ in the disk formation stage will be discussed later). Therefore, in

the below we give an indirect estimate of $|\dot{M}|$ the present model for the steady, viscous transonic solution allows.

In isothermal decretion, as in isothermal accretion, \dot{M} is not a parameter which characterizes the problem. It does not appear in the wind equations (8) and (9), so the absolute value of the surface density Σ is not determined from the model. Using the observed base density (i.e., the equatorial density at the inner disk radius $r = R$) to normalize Σ , however, we can estimate \dot{M} by

$$|\dot{M}| \sim 2 \times 10^{-11} \cdot \frac{\rho_{00}(R)}{10^{-11} \text{g cm}^{-3}} \cdot \frac{V_r(R)}{10^{-3} c_s} \times \left(\frac{T_d}{T_{\text{eff}}} \right)^{1/2} M_\odot \text{yr}^{-1}. \quad (15)$$

The base density, $\rho_{00}(R)$, for most stars analyzed from Fe II lines (Hanuschik 1986) and the IR excess (Waters et al. 1987; Dougherty et al. 1994) ranges from 10^{-11} to $10^{-12} \text{g cm}^{-3}$. Figure 1 shows that the radial velocity at the inner disk radius of the transonic decretion disks, $V_r(R)$, is roughly of the order of $10^{-3} \alpha c_s$, as far as the radiative force is much smaller than the gravity. As a result, we obtain $|\dot{M}|$ of the order of $10^{-11} - 10^{-12} \alpha M_\odot \text{yr}^{-1}$ for steady, viscous transonic disks.

It should be noted that this value does not increase very much even if we use $V_r(R)$ derived from the observed upper limit of the disk outflow velocity, i.e., a few km s^{-1} for $r \lesssim 10R$. Since V_r approximately linearly increases with r in viscous decretion disks, this upper limit of the disk outflow, $V_r(10R) < \text{a few km s}^{-1} \sim 0.1 c_s$, suggests that $V_r(R) \lesssim 10^{-2} c_s$ and $r_s \gtrsim 10^2 R$. Consequently, using the upper limit of the observed radial flow, we have $|\dot{M}| \sim 10^{-10} - 10^{-11} M_\odot \text{yr}^{-1}$ from equation (15). Our results, together with the observed range of the base density of Be disks, suggest that, in steady viscous decretion, the mass loss rate through the disk is at most comparable with that in the polar wind region.

It is interesting to note that another constraint on \dot{M} is obtained by estimating the spin-down timescale of the Be star. Porter (1998) derived the constraint on a quantity equivalent to \dot{M} , for which Be stars do not show significant spin-down during their main-sequence lifetimes. Porter adopted that each Be star loses its angular momentum at the rate of $|\dot{M}| \ell_K(R)$, where $\ell_K(R)$ is the Keplerian angular momentum at $r = R$ (here, for the sake of convenience, we have adopted the notation different from Porter's). In viscous disks, however, this rate is largely an underestimate, because it is likely that the Keplerian region extends at least up to $100R$ where the specific angular momentum is one order of magnitude larger than $\ell_K(R)$. Thus, we have to use $\sim 10 |\dot{M}| \ell_K(R)$ instead of $|\dot{M}| \ell_K(R)$ to evaluate the angular-momentum loss rate from the star. Then, the constraint for the star not to show significant spin-down during their lifetimes becomes more stringent than that derived by Porter (1998).

Since it is beyond the scope of the paper to present a detailed calculation, we roughly estimate the spin-down timescale below. For this purpose, we adopt the same stellar model as that adopted by Porter, i.e., a rigidly rotating polytrope with the index of $3/2$. The stellar angular momentum is, then, given by $\sim 0.2fM\ell_K(R)$, where f is the ratio of the stellar rotation velocity to the break-up velocity, which ranges from 0.4 for early Be stars to 0.8 for late Be stars. Then, the spin-down timescale is given by $\sim 0.2fM\ell_K(R)/10|\dot{M}|\ell_K(R) \sim 0.02fM/|\dot{M}| \sim 10^9(|\dot{M}|/10^{-10}M_\odot\text{yr}^{-1})\text{yr}$. Since the spin-down timescale has to be much longer than the main-sequence lifetime, which is $\sim 10^7\text{yr}$ for early Be stars and $\sim 10^8\text{yr}$ for late Be stars, we have the constraint on \dot{M} for Be stars: $|\dot{M}| \ll 10^{-8}M_\odot\text{yr}^{-1}$ for early Be stars and $|\dot{M}| \ll 10^{-9}M_\odot\text{yr}^{-1}$ for late Be stars. Since the observed disk structure of Be stars is insensitive to the spectral type, the latter constraint ($|\dot{M}| \ll 10^{-9}M_\odot\text{yr}^{-1}$) should be taken.

Observationally, the rate of equatorial mass loss has been derived for several stars only in the disk formation stage. Since 1977, μ Cen has exhibited only flickering emission caused by episodic mass loss events. Each outburst lasts only for 2–5 d and makes a transient, small disk which decays in 20–80 d. Hanuschik et al. (1993) estimated the mass loss rate for μ Cen during each outburst to be $4 \times 10^{-9}M_\odot\text{yr}^{-1}$. Recently, Telting et al. (1998) studied the long-term behavior of the Be disk in X Per (4U 0352+30), a Be/X-ray binary system, and derived the mass loss rate of $4 \times 10^{-9}M_\odot\text{yr}^{-1}$ during a disk build-up phase which lasted about 1 y in 1994–1995.

These values show that Be stars can eject mass at a rate much higher than the upper limit predicted by the viscous decretion model for steady disks. This suggests that the disk formation is a violent and, consequently, non-steady process to which the steady disk model cannot be applied. To study such a process, we need numerical simulations such as those by Kroll and Hanuschik (1997).

The short timescale of disk formation around these stars also suggests that the disk-formation process is essentially non-steady. For steady, viscous transonic disks shown in figure 1, the drift time defined by $\int_R^r V_r^{-1} dr$ is $\sim 30V_r(R)/10^{-3}c_s\text{yr}$ at $r = 10R$ and $\sim 80V_r(R)/10^{-3}c_s\text{yr}$ at the sonic radius. This means, even if $V_r(R)$ is as fast as $10^{-2}c_s$, the formation of an $r \sim 10R$ disk takes about 3 yr and that of a transonic disk takes about 8 yr. This long drift time suggests that only disks which are persistent for more than 10 yr will have the structure similar to those studied in this paper.

Next, we discuss the density distribution in Be disks. In isothermal decretion disks, the radial exponent of density, n , defined by $n = -d\ln\rho_{00}/d\ln r = -d\ln(\Sigma/H)/d\ln r$, is a little bit bigger than 3.5. More generally, as pointed out by Porter (1999), $2n + 3m \gtrsim 7$

must hold in order for the decretion to occur, where m is the radial exponent of the disk temperature. Since Be disks are roughly isothermal except for the very vicinity of the star (Millar, Marlborough 1998, 1999), we would expect that the observed density gradient index n is distributed around $n \sim 3.5$ with a small dispersion.

On the other hand, the observed values of n are distributed around $n \sim 3 - 3.5$, which is in agreement with the current model, with a dispersion much wider than that predicted. Adopting a simplified disk model, in which the disk has a constant opening angle and the density depends only on radius, and applying the curve of growth method by Waters (1986) to the observed far-IR excess for 59 Be stars, Waters et al. (1987) found $n = 2 - 4$. Adopting the same disk model as that of Waters et al. (1987), Dougherty et al. (1994) obtained $n = 2 - 5$ from the near-IR excess colors for 144 Be stars. Moreover, applying the curve of growth method with a more realistic disk model to a Be star, Porter (1999) obtained a value of n quite similar to that obtained by Waters et al. (1987).

Consequently, the viscous decretion disk model is roughly in agreement with the observed density distribution, but it has to explain why the observed density distribution ranges widely. In particular, the model has to explain why there are Be stars with $n \lesssim 3$, for which the decretion does not seem to occur. Porter (1999) pointed out that the viscosity dependent on the radius and/or the stellar radiation field may help make a decretion disk with a shallow density gradient. More detailed study of these possibilities is desired.

Finally, we come to the most important and long-standing issue to be solved, that is, the mechanism which enables a star to supply mass into the surrounding disk. Be stars rotate significantly slowly compared with the break-up velocities. Therefore, in order to supply mass, stars have to accelerate matter up to break-up velocities. Moreover, since most Be stars keep their disks for long periods, either the mass supply must be continuous or the interval of mass supply events must be much shorter than the viscous timescale. Otherwise, the disk would decay before the next mass supply event occurs, like the disk of μ Cen.

Although there is no widely-accepted mechanism for such mass supply, non-radial pulsations of stars may work. Osaki (1986) suggested that the dissipation of the non-radial pulsations gives matter the necessary angular momentum. Recently, Rivinius et al. (1997) found that in μ Cen the time interval of mass supply events is equal to a beat period of several strongest non-radial pulsation (NRP) modes, indicating that the mass supply from the star results from the resonance between strongest NRP modes. If this mechanism works in other Be stars, the frequencies of the strongest NRP modes in most Be stars will be distributed so that the beat period becomes much

shorter than the viscous timescale. It is highly desirable to study this possibility further.

The author is grateful for H.F. Henrichs, I. Negueruela, and J.M. Porter for stimulating discussions. He thanks the anonymous referee for useful comments. He also thanks the Astronomical Institute 'Anton Pannekoek', University of Amsterdam, for the warm hospitality, where during his stay most of this work was performed.

References

- Abott, D.C. 1982, *ApJ* 259, 282
 Abramowicz, M.A., Kato, S. 1989, *ApJ* 336, 304
 Allen, C.W. 1973, in *Astrophysical Quantities*, 3rd ed (The Athlone Press) London, pp206, 209
 Castor, J.I., Abott, D.C., Klein, R.I. 1975, *ApJ* 195, 157
 Chen, H., Marlborough, J.M. 1994, *ApJ* 427, 1005
 Dougherty, S.M., Waters, L.B.F.M., Burki, G., Coté, J., Cramer, N., Van Kerkwijk, M.H., Taylor, A.R. 1994, *A&A* 290, 609
 Ferrari, A., Trussoni, E., Rosner, R., Tsinganos, K., 1985, *ApJ* 294, 397
 Hanuschik, R.W. 1987, *A&A* 173, 299
 Hanuschik, R.W. 1994, in *Pulsation, Rotation and Mass Loss of Early-Type Stars*, IAU Symp 162, ed L.A. Balona, H. Henrichs, J.M. Le Contel (Kluwer Academic Publishers, Dordrecht) p265
 Hanuschik, R.W. 2000, in *The Be Phenomenon in Early-Type Stars*, IAU Colloq 175, ed M. Smith, H.F. Henrichs, J. Fabregat (ASP, San Francisco) in press
 Hanuschik, R.W., Dachs, J., Baudzus, M., Thimm, G. 1993, *A&A* 274, 356
 Hanuschik, R.W., Hummel, W., Dietle, O., Sutorios, E., 1995, *A&A* 300, 163
 Kato, S., Honma, F., Matsumoto, R. 1988, *MNRAS* 231, 37
 Kroll, P., Hanuschik, R.W. 1997, in *Accretion Phenomena and Related Outflows*, IAU Colloq 163, ed D.T. Wickramasinghe, G.V. Bicknell, L. Ferrario (ASP, San Francisco) p494
 Lee, U., Saio, H., Osaki, Y. 1991, *MNRAS* 250, 432
 Matsumoto, R., Kato, S., Fukue, J., Okazaki, A.T., 1984, *PASJ* 36, 71
 Millar, C.E., Marlborough, J.M. 1998, *ApJ* 494, 715
 Millar, C.E., Marlborough, J.M. 1999, *ApJ* 516, 276
 Negueruela, I., Okazaki, A.T. 2000, *A&A*, accepted
 Okazaki, A.T. 1991, *PASJ* 43, 75
 Osaki, Y. 1986, *PASP* 98, 30
 Papaloizou J.C., Savonije G.J., Henrichs H.F. 1992, *A&A* 265, L45
 Porter, J.M. 1998, *A&A* 333, L83
 Porter, J.M. 1999, *A&A* 348, 512
 Quirrenbach, K.S., Bjorkmann, K.S., Bjorkman, J.E., Hummel, C.A., Buscher, D.F., Armstrong, J.T., Mozukewich, D., Elias, N.M.II., Babler, B.L. 1997, *ApJ* 479, 477
 Rivinius, Th., Baade, D., Štefl, S., Stahl, O., Wolf, B., Kaufer, A. 1997, in *A Half Century of Stellar Pulsation Interpretations: A Tribute to Arthur N. Cox*, ed P.A. Bradley, J.A. Guzik (ASP, San Francisco) p343
 Snow, T.P. 1981, *ApJ* 251, 139
 Telting, J.H., Waters, L.B.F.M., Roche, P., Boogert, A.C.A., Clark, J.S., de Martino, D., Persi, P. 1998, *A&A* 296, 785
 Waters, L.B.F.M. 1986, *A&A* 162, 121
 Waters, L.B.F.M., Coté, J., Lamers, H.J.G.L.M. 1987, *A&A* 185, 206
 Waters, L.B.F.M., Marlborough, J.M. 1994, in *Pulsation, Rotation and Mass Loss of Early-Type Stars*, IAU Symp 162, ed L.A. Balona, H. Henrichs, J.M. Le Contel (Kluwer Academic Publishers, Dordrecht) p399